Design of Intelligent Management Technology for Hotel Air Conditioning Based on Coupling Model and Deep Neural Network

Yunzi Gu
Tourism and Management Department, Wuhan College of Foreign Language and Foreign Affairs, Wuhan 430205, China
E-mail: collencollencollen@163.com

Keywords: deep belief network, VAV, temperature and humidity prediction control, building heat transfer characteristics, hotel air conditioning

Received: May 9, 2024

Variable air volume air conditioning systems have the advantages of low energy consumption and easy control, making them an important object in the field of air conditioning. This study uses deep belief networks to predict and control the temperature and humidity of variable air volume air conditioning systems in hotel buildings. It analyzes the heat transfer characteristics of building envelope structures by constructing mathematical models and optimizes deep belief network models to improve prediction accuracy. By using the proportional integral control algorithm, the system dynamically adjusts the air valve based on the difference between the predicted indoor temperature and the set target temperature, achieving precise control of the indoor environment. The results showed that indoor temperature could quickly adapt to outdoor temperature changes, and the average absolute relative error of the deep belief network model was 1.555%, with a determination coefficient of 0.9975. In practical applications, the room temperature successfully reached the predetermined target within 300 minutes, maintaining stability even in the presence of interference. The research results provide an efficient intelligent control method for building energy management.

Povzetek: Študija se osredotoča na načrtovanje inteligentne tehnologije upravljanja hotelske klimatske naprave z uporabo modela spajanja in globokih nevronskih mrež. Prispevek izboljšuje napovedovanje temperature in vlažnosti ter omogoča učinkovito upravljanje notranjega okolja.

1 Introduction

With the increasing global energy consumption, building energy consumption has become an important component, among which Heating, Ventilation, and Air Conditioning (HVAC) systems account for a significant share of building energy consumption [1]. Especially in large public buildings such as hotels, the energy consumption problem of Air Conditioning Systems (ACS) is particularly prominent due to their special usage needs and complex spatial structures [2]. Traditional air conditioning control methods often rely on fixed parameter settings, which are difficult to adapt to the changing load demands and environmental changes inside hotels, resulting in energy waste and a decrease in indoor environmental comfort [3]. The Temperature and Humidity (T&H) control strategy for a single area cannot effectively address the complexity of multi-area ACSs in actual operation, especially in large hotel buildings where there are significant differences in air conditioning demand and environmental response in different areas. In addition, traditional methods often find it difficult to achieve precise control when dealing with nonlinear, strongly coupled, and large lag ACSs. There are problems such as debugging difficulties and slow response in practical applications [4-5]. Therefore, this study proposes a hotel air conditioning Intelligent Management Technology (IMT) based on a coupled model and Deep Neural Network (DNN). By establishing a T&H coupling model for multi-area Variable Air Volume (VAV) Air Conditioning System (VAV-ACS) in buildings, it is possible to more accurately simulate and predict changes in the indoor environment. The innovation of the research lies in combining coupled models with deep learning techniques, which can improve the accuracy and response speed of ACS control. This study also introduces Fuzzy Clustering Algorithms (FCA), with the objective of enabling the ACS to adaptively adjust its operating strategy to adapt to the constantly changing indoor and outdoor environments and user needs.

The study consists of four parts. Part 1 is a summary of existing research. Part 2 is the analysis of the characteristics of hotel building ACSs and the IMT study of DNN. Part 3 is the analysis and experimental verification of the temperature control effect of the VAV-ACS based on FCA. Part 4 summarizes the entire text.

2 Related works

Scholars such as He et al. proposed a new parameter tuning method that combines machine learning and

improved Particle Swarm Optimization (PSO) to address the difficulty in optimizing MPC controller parameters in VAV-ACS. The method established the relationship between parameters and performance indicators through machine learning, and then used PSO for parameter optimization to improve system response. Meanwhile, the PSO algorithm had been improved through population decay and event triggering, effectively reducing computation time [6]. Zhao et al. explored the feasibility and economic benefits of combining DOAS with ventilation system renovation while retaining the original VAV system. They also compared the performance of VAV-DOAS with traditional VAV under the multi-space equation strategy. The experiment showed that VAV-DOAS could save 16% and 21% energy in winter and summer seasons in Dalian area [7]. Nassif and Ridwana explored the potential of dual VAV systems in building energy efficiency and proposed a new control strategy to effectively distribute cooling loads by using the heating ducts of the system as dedicated outdoor air units. This system could significantly reduce fan power and heating energy consumption by simulating the performance of single-duct and double-duct VAV systems in different building scenarios, while having a relatively small impact on refrigeration load [8]. Zhao et al. compared constant and variable Outdoor Air Flow Ratio Strategies (OAFRS). The results showed that both strategies had the same effect on indoor air quality control, but the variable strategy could better adapt to changes in occupancy. In terms of energy consumption, the strategy based on multiple space equations saved 6.76% and 9.88% in heating and cooling seasons, respectively, compared to the maximum OAFRS [9]. Zhao et al. analyzed the distribution and mutual interference of pressure and airflow in pipeline networks under DP and FF strategies through MATLAB simulation. Compared to DP strategy, FF could reduce damper position changes, reduce pressure and airflow fluctuations [10].

Researchers such as Jornet-Monteverde and Galiana-Merino designed a controller module and a node module to communicate with the touch screen interface through the MQTT protocol. They constructed a Wi-Fi network using the CC3200 micro-controller, TI-RTOS system, and Raspberry Pi. The system could save energy by 75% -94% when used in a single area and 44% when used in a whole house, significantly improving energy efficiency and user comfort [11]. Wei et al. developed a VAV system model predictive control framework based on Artificial Neural Networks (ANN). Through the collaborative work of ANN controller and PI controller, the control of regional temperature, dampers, and Air Supply Volume (ASV) had been optimized. By using the Lagrangian variational method for online optimization, the energy efficiency of the system was improved by 6.12% after considering the wind turbine control signal [12]. Yu et al. proposed a control algorithm based on multi-agent deep reinforcement learning and attention mechanism to address the issue of high energy consumption in HVAC systems in commercial buildings. It transformed the problem of minimizing energy costs into a Markov game, which can be operated without prior knowledge or building thermodynamic models. Simulation showed that this algorithm could effectively reduce energy costs while ensuring thermal comfort and indoor air quality [13]. Zhao et al. explored the application of data mining technology in building energy systems through a comprehensive literature review. This study divided data mining techniques into two categories: supervised and unsupervised, which were respectively used for energy load forecasting, fault diagnosis, and operation mode recognition [14].

Table 1: Summary table of related work

Authors	Methodology	Application	Results	Limitations
He et al. [6]	Machine Learning + Improved PSO	VAV System Controller Parameter Optimization	Enhanced system response, reduced computation time	Specific application scenarios or actual effects not mentioned
Zhao et al. [7]	Integration of VAV and DOAS	Ventilation System Retrofitting	Energy savings of 16% in winter and 21% in summer	Study limited to Dalian area, may not be generalizable
Nassif and Ridwana [8]	Dual VAV System Control Strategy	Building Energy Conservation	Reduced fan power and heating energy consumption, minimal impact on cooling load	Impact on indoor comfort levels not mentioned
Zhao et al. [9]	Multi-zone Equation Strategy	Indoor Air Quality Control	Significant energy savings, equivalent indoor air quality control as constant strategy	Research may be limited to specific building types and climate conditions

Jornet-Monteverde and Galiana-Merino [11]	MQTT Protocol, CC3200 Micro-controller, etc.	Wi-Fi Network Control	Energy savings of 75%-94% in single-zone, 44% in whole-house	Long-term stability and scalability not mentioned
Wei et al. [12]	ANN Model Predictive Control Framework	VAV System	6.12% increase in system efficiency	Need further verification of the algorithm's performance in different building environments
Yu et al. [13]	Multi-agent Deep Reinforcement Learning	Commercial Building HVAC System	Effectively reduced energy costs, ensured thermal comfort and indoor air quality	Algorithm complexity may require substantial computational resources
Zhao et al. [14]	Data Mining Techniques	Building Energy Systems	Energy load prediction, fault diagnosis, etc.	Literature review study, no specific application case provided

In summary, there are still shortcomings in the parameter optimization, system response speed, energy consumption, and control strategy flexibility of VAV-ACS in existing research. Despite the application of machine learning and optimization algorithms, the parameter optimization process still faces challenges in adaptability and efficiency. The existing system has limited performance in quickly responding to environmental changes to maintain indoor comfort. In addition, although some studies have shown energy-saving potential, energy consumption remains high in multiple regions and large public buildings [15]. The existing control strategies need to improve their adaptability and flexibility to cope with complex and ever-changing building load demands. Therefore, this study introduces IMT based on coupled models and DNNs to improve prediction accuracy, accelerate response speed, reduce energy consumption, and enhance the flexibility of control strategies. The aim is to provide significant technological progress for the field of building energy management.

3 Analysis of ACS characteristics in hotel buildings and IMT study of DNN

This chapter describes the ACS characteristics of hotel buildings, including room structure and T&H control in public areas, and establishes a mathematical model to simulate the indoor environment. Additionally, it presents the IMT of the VAV system based on DNN, which enables precise control of the air conditioning supply volume through the construction of predictive models and the optimization of control strategies. This results in enhanced energy efficiency and improved indoor comfort.

3.1 Establishment of a coupled model for indoor air parameters in hotels

This study focuses on the ACS of hotel buildings, where the room sizes are relatively consistent and the environmental parameters of public corridors are easy to measure, with standard rooms accounting for the majority, as shown in Figure 1.

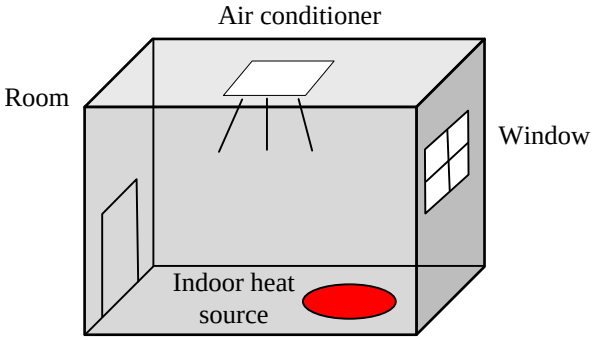

(a) Typical room mathematical model

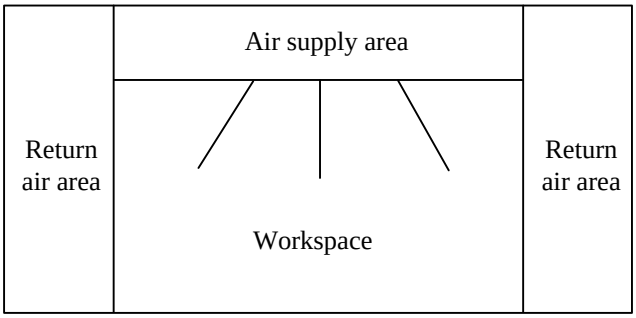

(b) Air conditioning air supply area division map

Figure 1: Typical room mathematical model and air conditioning ASA division diagram

In Figure 1 (a), the hotel room consists of six interfaces. One external wall is in direct contact with the outside world, including walls and windows. The inner wall is adjacent to the corridor and usually has doors. The ceiling and floor form the upper and lower sides. On both sides are walls that connect with adjacent rooms. The VAV-ACS terminal equipment is installed inside the room. As shown in Figure 1 (b), before establishing a single room T&H coupling mathematical model, this study assumes that the air in the room can be simplified into a particle, facilitating the application of energy balance theory. Meanwhile, walls and floors can be considered as multi-layer structures, with the Heat Capacity (HC) and resistance concentrated on specific particles to establish an Energy Balance Equation (EBE). A mathematical model is constructed to analyze the heat transfer characteristics of the hotel ACS. To simplify the calculation, the heat transfer coefficient is assumed to be constant, although this may be affected by environmental changes. Sensitivity analysis is used to evaluate the potential impact of this assumption on the accuracy of the predictions. The model further refines the heat transfer simulation of the multi-layer structure of the wall and floor, and adopts an RC network model to improve the simulation accuracy. Using the RC network model, the walls and floors of the enclosure structure are divided into two layers, each consisting of four EBEs. The EBE for the outer surface of the wall is equation (1).

$$\begin{aligned} &4A_{wa}K_{wa}(T_{wa2}-T_{wa,out})+\\ &A_{wa}K_{wa,out}(T_{out}-T_{wa,out})=0 \end{aligned} \tag{1}$$

In equation (1), A_{wa}, K_{wa}, T_{wa2}, and $T_{wa,out}$ represent the area of the wall, Heat Transfer Coefficient (HTC), second node temperature, and outer Surface Temperature (ST). $K_{wa,out}$ represents the HTC between the outdoor air and the surface area of the wall. T_{out} represents the outdoor air temperature. The EBE for the first node of the wall is equation (2).

$$\begin{aligned} &\frac{1}{2}\rho_{wa}\delta_{wa}A_{wa}C_{wa}\frac{dT_{wa2}}{dt}=\\ &2A_{wa}K_{wa}\left(T_{wa1}-T_{wa2}\right)+4A_{wa}K_{wa}\left(T_{wa,out}-T_{wa2}\right) \end{aligned} \tag{2}$$

In equation (2), ρ_{wa}, δ_{wa}, and C_{wa} are the density, thickness, and HC. The EBE for the wall's second node is equation (3).

$$\begin{aligned} &\frac{1}{2}\rho_{wa}\delta_{wa}A_{wa}C_{wa}\frac{dT_{wa1}}{dt}=\\ &4A_{wa}K_{wa}\left(T_{wa,out}-T_{wa1}\right)+2A_{wa}K_{wa}\left(T_{wa2}-T_{wa1}\right) \end{aligned} \tag{3}$$

Finally, the EBE for the inner surface is equation (4).

$$\begin{aligned} &4A_{wa}K_{wa}\left(T_{wa1}-T_{wa,in}\right)+\\ &A_{wa}K_{wa,in}\left(T_{inr}-T_{wa,in}\right)=0 \end{aligned} \tag{4}$$

In equation (4), $T_{wa,in}$ represents the inner ST, and T_{inr} represents the air temperature in the return air area. The air balance equation for indoor work areas is equation (5).

$$\begin{aligned} &\left(\rho_a V_{ins}C_a+C_f\right)\frac{dT_{ins}}{dt}=K_{wa,in}A_{wa,w}\left(T_{wa,in}-T_{inw}\right)\\ &+K_{win}A_{win}\left(T_{out}-T_{inw}\right)+K_{fl,in}A_{fl,w}\left(T_{fl,in}-T_{inw}\right)\\ &+G_{sa}C_a\left(T_{sa}-T_{inw}\right)+\sum_i \rho_a V_{adj,i}C_a R\left(T_{adj,i}-T_{inw}\right)\\ &+A_{la}K_{la}\left(T_{la}-T_{inw}\right) \end{aligned} \tag{5}$$

In equation (5), C_a and C_a represent the air HC of the blowing-in area and the working area. T_{inw} and $T_{adj,i}$ are the air temperature in the indoor workspace and adjacent rooms. $K_{fl,in}$ represents the HTC between the inner surface of the roof and the indoor air. $A_{fl,w}$ and $T_{fl,in}$ are the area of the roof and the internal ST. G_{sa} is the air supply mass flow rate. T_{sa} represents the supply air temperature. ρ_a represents the air density in the workspace. K_{la} and T_{la} are the HTC and temperature of the indoor heat source. The indoor air humidity and enthalpy balance equation is equation (6).

$$\begin{aligned} &\rho_a V_{inw}\frac{dT_{inw}}{dt}=G_{sa,sw}\left(h_{sa}-h_{inw}\right)+\\ &K_{wa,in}A_{wa,w}\left(T_{wa,in}-T_{inw}\right)+\\ &K_{win}A_{win}\left(T_{out}-T_{inw}\right)+\\ &K_{fl,in}A_{fl,w}\left(T_{fl,in}-T_{inw}\right)\\ &+K_f A_f\left(T_f-T_{inw}\right)+\\ &\sum_i \rho_a V_{adj,i}C_a R\left(T_{adj,i}-T_{inw}\right)+\\ &A_{la}K_{la}\left(T_{la}-T_{inw}\right) \end{aligned} \tag{6}$$

In equation (6), h_{sa} and h_{inw} are the enthalpy values of the supply air and indoor air. The humidity balance equation for indoor work areas is equation (7).

$$\begin{aligned} &V_{inw}\rho_a\frac{dM_{inw}}{dt}=G_{sa,sw}M_{ins}-G_{sa,sw}M_{inw}\\ &+\sum_i \rho_a V_{adj}R\left(M_{adj,i}-M_{inw}\right) \end{aligned} \tag{7}$$

In equation (7), M_{inw} and M_{ins} represent the air humidity in the indoor work area and indoor Air Supply Area (ASA). $M_{sa,sw}$ represents the humidity of the air supply from the ASA to the work area. $G_{sa,sw}$ represents the air supply quality flow rate between the ASA and the work area. V_{inw} represents the volume of the workspace. In hotels with corridors, the first floor often has a spacious lobby, which is typically supplied with air by multiple Variable Air Volume Boxes (VAVB). These VAVBs will interact with each other during operation, leading to coupling of air flow. The working area of the air conditioner is shown in Figure 2.

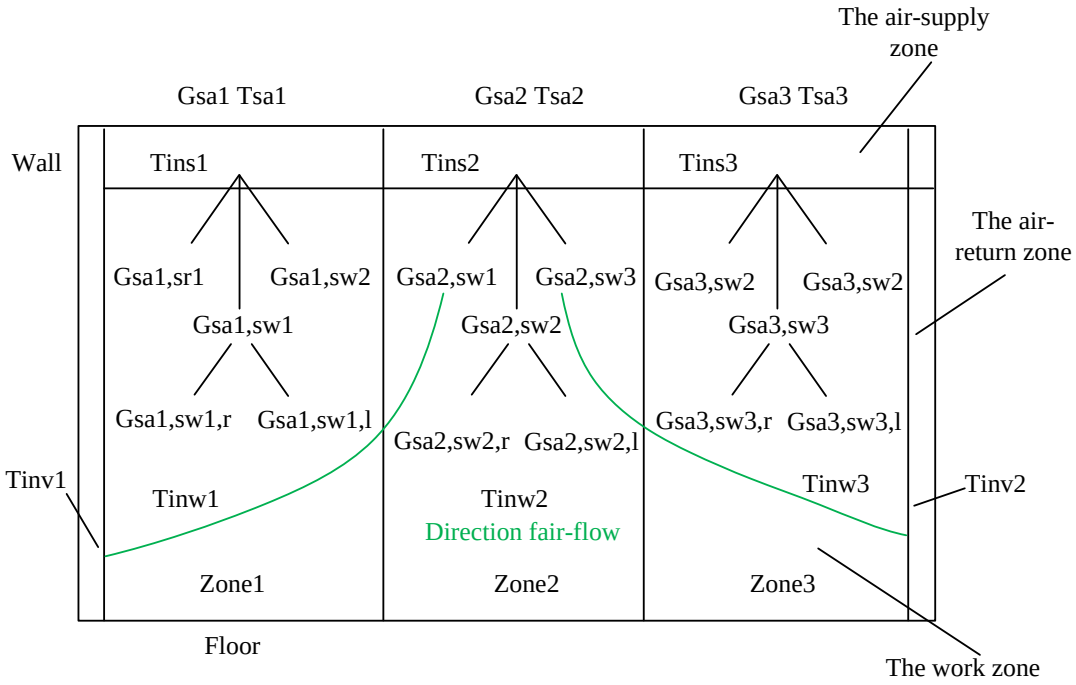

Figure 2: Air-conditioned work area

In multi-zone rooms, air typically flows between spaces through windows and doors. During this process, indoor air exchanges energy and mass with the surrounding environment, following the principle of mass conservation, and the total air flowing in and out of each room remains constant [16-17]. Therefore, this study divides the building into N areas. Considering the diversity of room structures, it is assumed that every room owns M interfaces, which means there have multiple shared interfaces in the entire building. For any two regions i and j, the air flow exchange between them is equation (8).

$$q^{i-j} = f\left(\Delta P^{i-j}\right) \tag{8}$$

Taking any area i within a multi-area building, according to the law of conservation of mass, equation (9) is obtained.

$$\begin{cases} \dfrac{\partial m_i}{\partial t} = \rho_i \dfrac{\partial V_i}{\partial t} + V_i \dfrac{\partial \rho_i}{\partial t} = \sum_{k=1}^{n} f\left(\rho_k, \rho_i\right) \cdot q^{i-k} \\ f\left(\rho_k, \rho_i\right) = p_k \Delta P > 0 or p_i \Delta P < 0 \end{cases} \tag{9}$$

In equation (9), m_i and ρ_i represent the air quality and air density in region i. ρ_k indicates the air density within the adjacent area k of i. V_i is the i's volume. q^{i-k} represents the air permeability through the k-th wall of i. $f\left(\rho_k, \rho_i\right)$ is the density value function. For multi-area buildings, each room also satisfies the Mass-action law, as shown in equation (10).

$$F\left(P_t\right) = 0 \tag{10}$$

According to the coupling model, the air flow in each area of a large space room with multiple VAVB can be solved for indoor air flow coupling [18]. The mathematical model of single room T&H coupling is equation (11).

$$CX^{'} = AX + BU \tag{11}$$

In addition, it can be assumed that the walls and floors are divided into two layers, and the room can be divided into supply air area, work area, and return air area according to the function of ACS to more accurately simulate and control the indoor environment. VAV-ACS consists of five core components, including intelligent automatic control system, Air Handling Unit (AHU), air conveying unit, ventilation duct, and air conditioning terminal device. These components work together to achieve efficient operation of the system, and the specific structural layout can be seen in Figure 3.

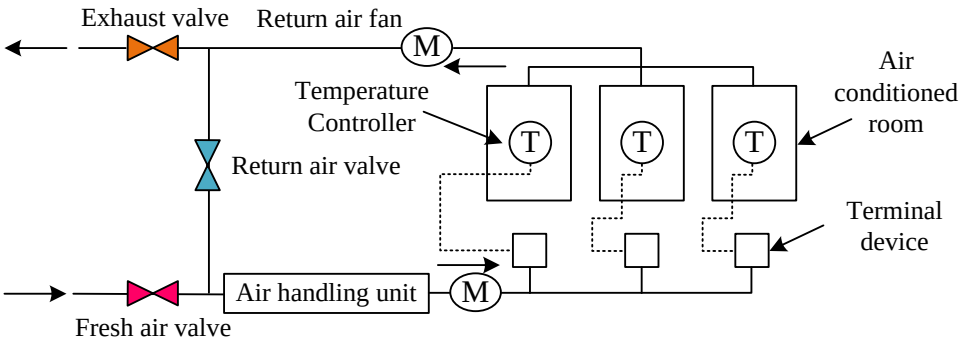

Figure 3: Schematic diagram of VAV-ACS

ACS consists of multiple key components, including air handling equipment located at the top of the building, which is responsible for adjusting fan speed to control air supply and meet room requirements. Air conveying equipment ensures effective air distribution by adjusting the opening of the air supply valve and providing circulating power. As a ventilation duct, the air duct system needs to have appropriate strength and air-tightness to prevent air leakage and noise. The air conditioning terminal device directly affects Indoor Temperature (InT) and comfort, and maintains the ideal indoor environment by adjusting the ASV. Finally, as the core of VAV-ACS, the automatic control system ensures comfort and improves energy efficiency by monitoring and controlling various parameters. These components work together to ensure efficient and energy-efficient operation of ACS.

3.2 Air conditioning airflow analysis and IMT based on DNN

VAV system, also known as VAV-ACS, is a solution that utilizes all air conditioning to regulate indoor environments. The system adjusts the amount of air sent into the room to meet the heat load and humidity requirements of different areas, ensuring that the indoor environment meets the predetermined comfort standards [19-20]. The VAV system can dynamically adjust the fan

speed and valve opening of the end device based on actual load changes, while transmitting operating data and control feedback information to the air conditioning control system. The VAV control diagram is shown in Figure 4.

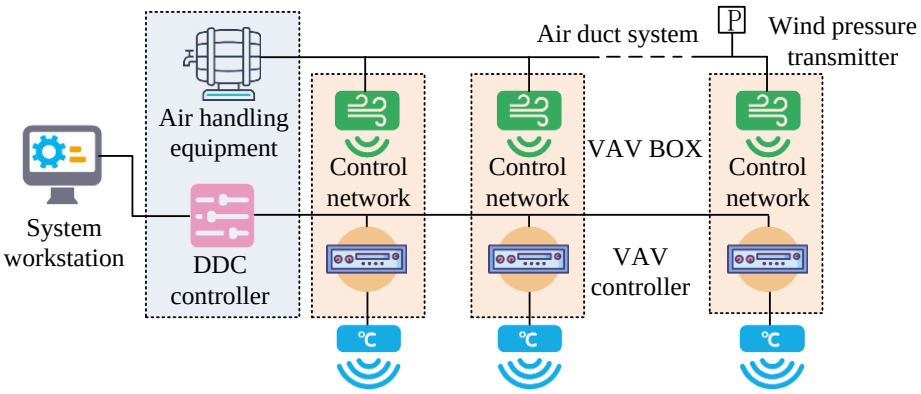

Figure 4: VAV control char

In VAV-ACS, the air conditioning unit controls the ASV by adjusting the variable frequency current to meet the needs of different rooms. The VAV BOX terminal device is carefully arranged in various rooms, and the Air Volume (AV) of the air supply outlet is controlled by adjusting the air valve opening, achieving precise management of indoor T&H. These devices can respond to changes in the indoor environment and automatically adjust the air supply to maintain a set level of comfort. In the air conditioning design of the hotel, each room is equipped with a temperature regulator, which achieves temperature regulation and detection through VAV BOX end devices. When there is a deviation between the InT and the preset value, the end device will measure the difference and adjust the ASV to correct it. The detection function of VAV BOX can also monitor the ASV to ensure it is consistent with the set value. If there is any deviation, it can be corrected by adjusting the intake valve. VAV BOX consists of a casing, controller, and actuator to ensure the efficient operation of ACS.

To build a predictive model for VAV Supply Air Volume (VAV-SAV), it is necessary to first create a training dataset. This dataset takes the actual VAV-SAV at a specific time t as the output, and includes the SAV at the same time in the previous time and day, Outdoor Temperature (OuT) at the same time and its data from the previous day and two days, solar radiation and atmospheric humidity on that day as input features. These features together form the training set S. Then the training set S is input into the Deep Belief Network (DBN) model. The training of DBN adopts a layer-by-layer pre-training and fine-tuning strategy. In the pre-training stage, the Contrastive Divergence algorithm is used, which is a first-order form of contrastive divergence. The Restricted Boltzmann Machine (RBM) is trained layer by layer in an unsupervised manner. In the fine-tuning stage, the Back Propagation (BP) algorithm is used to perform supervised fine-tuning on the entire network. To predict VAV-SAV in the new dataset D, the test samples are input into the trained DBN model, which will output the predicted ASV y. In the training phase of DBN, the initial restricted RBM first generates a feature vector in the input layer, which is then passed to the hidden layer. Through this process, the network can attempt to reconstruct the data of the input layer. The training process of DBN is detailed in Figure 5.

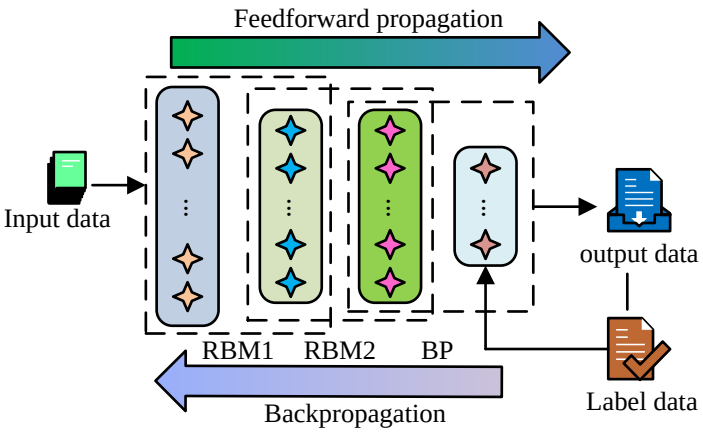

Figure 5: DBN training process

To ensure the accuracy of the prediction results, the research model makes detailed parameter adjustments to the network structure. The model design includes two hidden layers and employs empirical formulas to optimize performance, as shown in equation (12).

$$\sum_{i}^{n} C_M^i > k \tag{12}$$

In equation (12), n represents the number of neurons in the input layer, M represents the number of neurons in the hidden layer, and k represents the number of samples. If $i > M$, then $C_M^i = 0$, equation (13) can be obtained.

$$M = (n+m)^{1/2} + a \tag{13}$$

In equation (13), m represents the number of neurons in the output layer, and a represents the constant between $[0,10]$, which leads to the equation (14).

$$\begin{cases} M = \log_2 n \\ M = (mn)^{1/2} \end{cases} \tag{14}$$

According to equation (14), the final expression of M can be derived, as shown in equation (15).

$$M = \left(0.43mn + 0.12m^2 + 2.54n + 0.77m + 0.86\right)^{1/2} \tag{15}$$

According to equation (15) and continuous debugging of the number and learning rate of hidden layer neurons during the simulation process, 14 neurons are selected for the first layer and 7 neurons for the second layer. This study uses FCA to optimize the model, and the optimized model is displayed in Figure 6.

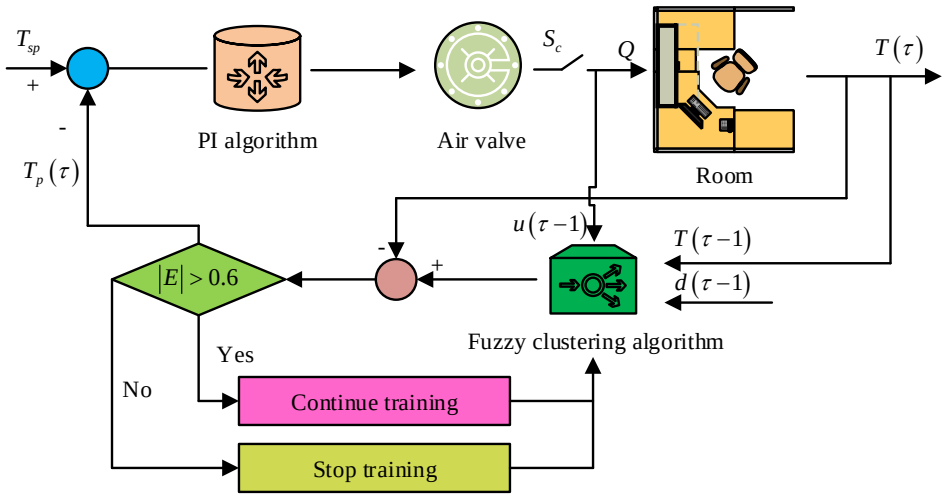

Figure 6: Predictive control model of room temperature time-delay system based on FCA

In Figure 6, y_{sp} is the set temperature value. $u(\tau-1), y(\tau-1), y'(\tau-1), d(\tau-1)$ are the first derivative and disturbance of the input, output, and output of the system at time $\tau-1$ of the model. y_p is the predicted value of room temperature. Q is the ASV of the room. E is the deviation between the predicted InT and the set value. Sc is the control period. After training to $|E| \le 0.6$, FCA can describe the dynamic features of delayed time system. In the study, the InT predicted by the network model is used as input for the control cycle to replace the actual room temperature output. These predicted values are used for the next round of system iteration. The system adjusts the opening of the air valve through PI control algorithm based on the difference between the predicted temperature and the target temperature to maintain InT. During the implementation process, the system regularly collects key parameters such as valve position and fan speed, and then uses FCA to predict room temperature. Based on the prediction results, the valve is adjusted in real-time to accurately control the indoor environment.

4 Analysis and experimental verification of temperature control effect of VAV-ACS based on FCA

This study conducts simulation experiments based on the developed single room T&H coupling model. These experiments exclude the impact of indoor personnel activities and focus on analyzing the effect of building

envelope structures on indoor environmental loads. In the experiment, the VAV-ACS optimized by DBNs sets an InT target of 22℃. The initial setting of the air valve opening is 30%, and dynamic adjustment of the indoor and outdoor temperature deviation is carried out every 5 minutes according to the PI algorithm. The system components include an air handling unit with a rated air volume of 1500 m3/h and conveying equipment. Real-time monitoring of key operating parameters is implemented, and FCA is used to optimize the adjustment of air valves to adapt to environmental changes. The experiment is conducted under stable outdoor temperature conditions, with an approximate mean of 25℃, from 10:00 PM to 3:00 PM each day. This ensures consistency in the experimental environment. Prior to the experiment, the room temperature is set at 20℃ and maintains for 20 minutes. The key hyper-parameters include a learning rate of 0.01, batch size of 64, iteration count of 1000, as well as 500 neurons in the first hidden layer and 250 neurons in the second layer of the network structure. During the training process, a cross entropy loss function and a stochastic gradient descent method with a momentum of 0.9 are used to optimize network performance and generalization ability. To validate the model, this study simulates two different operating conditions in MATLAB software. The building envelope structure parameters and corresponding indoor and outdoor environmental conditions for these working conditions are detailed in Table 2, aiming to observe and compare the dynamic changes of indoor T&H under different conditions.

Table 2: Building envelope parameters and indoor and outdoor data of environment

Different parameters	Working condition one	Working condition two
Wall HTC	$K_{wa}=0.5W/\left(m^2°C\right)$	$K_{wa}=1.2W/\left(m^2°C\right)$
HTC of inner surface of wall	$K_{wa,in}=5W/\left(m^2°C\right)$	$K_{wa,in}=6.5W/\left(m^2°C\right)$
Roof HTC	$K_{fl}=2W/\left(m^2°C\right)$	$K_{fl}=1.2W/\left(m^2°C\right)$
Window HTC	$K_{win}=3W/\left(m^2°C\right)$	$K_{win}=3.2W/\left(m^2°C\right)$
Wall outer ST	$T_{wa,out}=0°C$	$T_{wa,out}=-6°C$
HTC of wall outer surface	$K_{wa,out}=12W/\left(m^2°C\right)$	$K_{wa,out}=12.5W/\left(m^2°C\right)$
Roof outer surface HTC	$K_{fl,out}=6W/\left(m^2°C\right)$	$K_{fl,out}=6.5W/\left(m^2°C\right)$
Roof exterior ST	$T_{fl,out}=0°C$	$T_{fl,out}=6°C$

Figure 7 shows the temperature response curves under operating conditions 1 and 2.

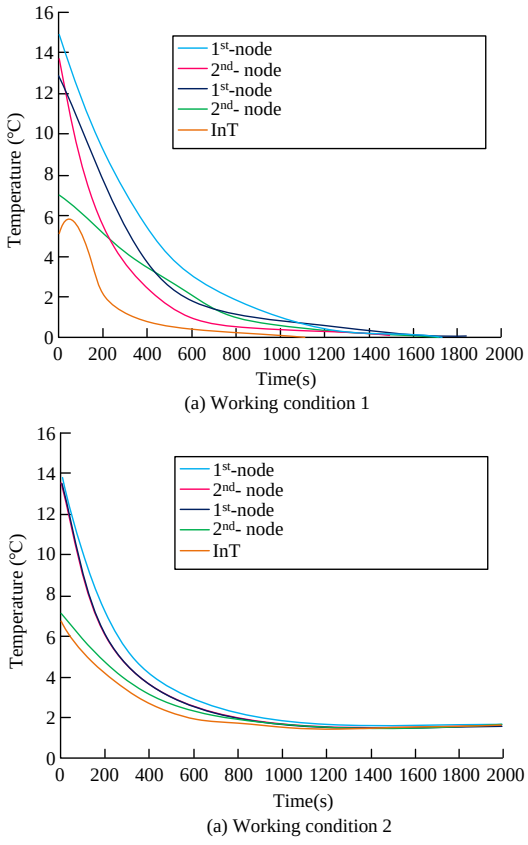

(a) Working condition 1

(a) Working condition 2

Figure 7: Response curves under different temperature conditions

In Figure 7, this study observed the changes in building structure (including walls and floors) and Indoor Air Temperature (IAT), with no heat source and no heating provided indoors. In Figure 7 (a), under operating condition one, the initial IAT was 5 °C, which dropped to 0 °C after 800 seconds, which was equal to the OuT. The temperature nodes of the walls and roofs also reached the OuT within the same time. In Figure 7 (b), in operating condition 2, the initial IAT was slightly higher at 7 °C, but it also dropped to -6 °C after 800 seconds, consistent with the OuT. Therefore, regardless of operating conditions 1 or 2, the temperature nodes of IAT and the building structure reached the same temperature level as the outdoor environment after 800 seconds. This indicated that in the absence of internal heat sources and heating, IAT would quickly adjust to the OuT. To verify the effectiveness of the research model, actual air supply data and outdoor meteorological data of a large VAV-ACS were collected for predictive analysis. The comparison of prediction errors of different neural network models is shown in Figure 8.

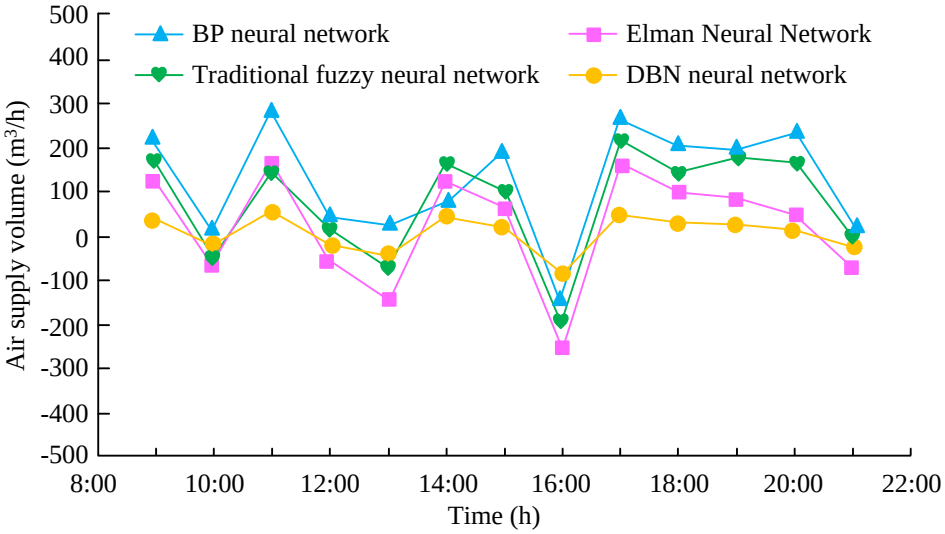

Figure 8: Comparison of prediction errors of different neural network models

In Figure 8, the DBN model had a significant advantage in prediction accuracy, showing higher stability and accuracy in hourly air supply prediction, effectively avoiding the local convergence and over-fitting problems that traditional neural networks may encounter. The Mean Absolute Relative Error (MARE), root mean square relative error, and coefficient of determination reached 1.555%, 0.789%, and 0.9975, respectively. Therefore, the DBN model had the smallest error and more stable volatility compared to BP, Elman, and fuzzy models, providing the best predictive performance. This study selected three rooms from a certain hotel for actual measurement. Table 3 shows the VAV-ACS electromechanical equipment data.

Table 3: VAV-ACS electromechanical equipment parameters

Device name	Specification (AV)
AHU	1500 m3/h; Rated cooling capacity: 10 kW
Ventilator	1500 m3/h; Rated power: 5kW
Terminal control device 1	0-315 m3/h
Terminal control unit 2	0-315 m3/h
Terminal control 3	0-315 m3/h

Considering the differences in the enclosure structures of the three rooms in the experimental platform, this study chose Room 1 and Room 3 as the experimental subjects. To ensure the stability of the experimental conditions and avoid interference from outdoor environmental changes, the experiment was scheduled to be conducted between 10:00 pm and 3:00 pm every day. Before the experiment begins, assuming that the temperature inside the laboratory and the end SAV remained constant for a certain period of time. The PI algorithm was used to control the VAV-ACS chilled water valve to maintain the supply air temperature within the preset range. During the dynamic adjustment process of VAV-ACS, the opening of the end air valve in the same room was kept consistent to accurately observe and analyze the dynamic response. The effect of VAVB

damper adjustment on the temperature of three rooms is displayed in Figure 9.

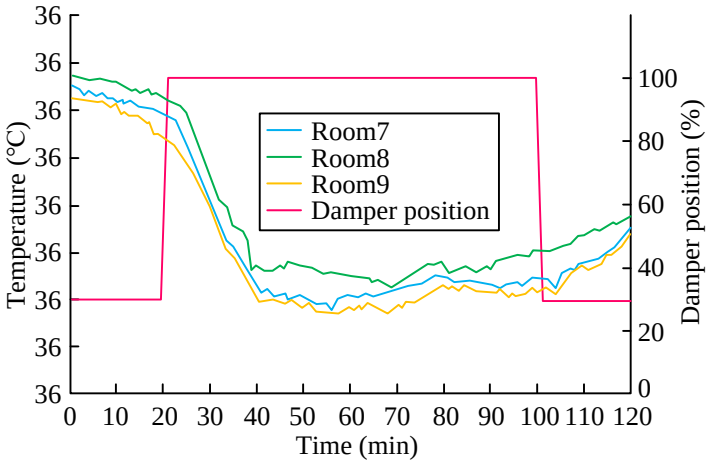

(a) Indoor temperature response curve under summer conditions

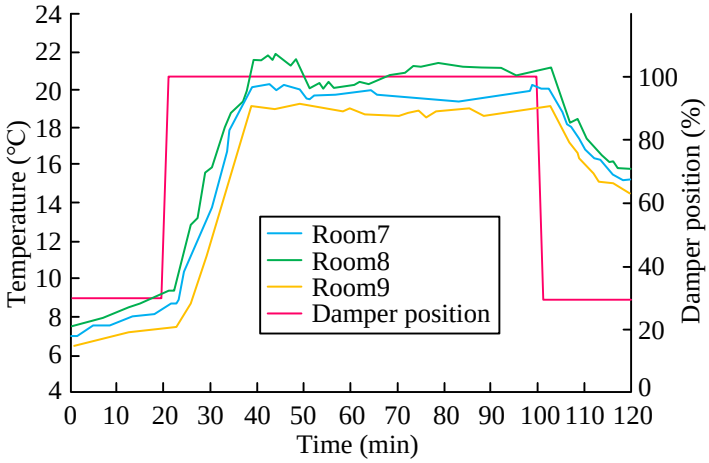

(b) Indoor temperature response curve under winter conditions

Figure 9: Effect of VAVB damper adjustment on the temperatures of three rooms

Figure 9 showed the effect of VAVB damper adjustment on the temperature of three rooms in different seasons. In Figure 9 (a), during summer, the starting temperatures of rooms 7, 8, and 9 were 33 °C, 33.5 °C, and 32.5 °C, respectively. The damper opening increased from 30% to 100% at 20min, causing a significant decrease in room temperature at 24min and stabilizing at 40min. When the air door opening decreased to 30% at 100 minutes, the room temperature increased significantly at 104min, and by 120min, the temperatures in the three rooms dropped to 27 °C, 27.5 °C, and 26.8 °C, respectively. In Figure 9 (b), the winter situation was similar, with room starting temperatures of 7 °C, 7.5 °C, and 6.5 °C. The adjustment of the damper opening also caused a significant change in room temperature at 24min and stabilized at 40min. The readjustment of the damper opening was carried out at 100min, resulting in a rapid change in room temperature after 104min. Finally, at 120min, the temperatures of the three rooms were adjusted to 15.2 °C, 15.8 °C, and 14.6 °C, respectively. The data showed that there was a delay of approximately 4min in the response of InT to the adjustment of air door opening. The control effect of FCA is shown in Figure 10.

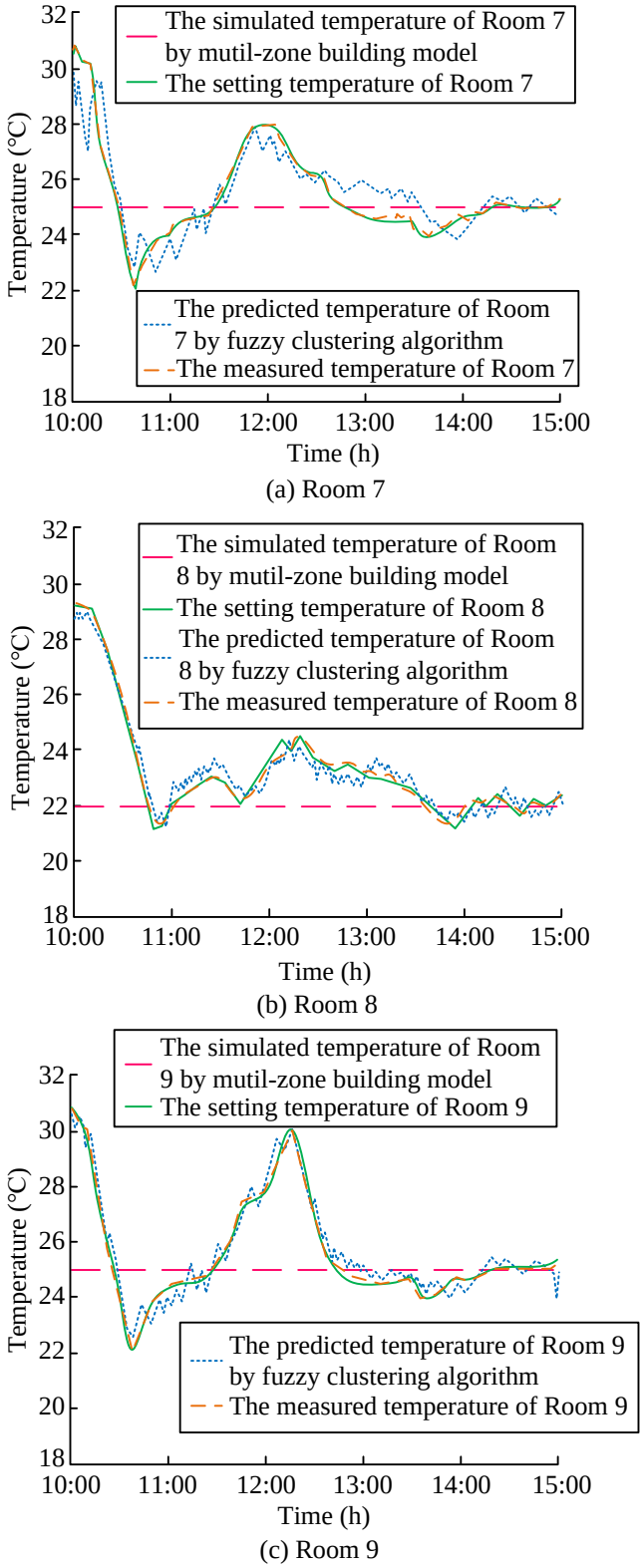

Figure 10: Room temperature control effects in different rooms

Figures 10 (a), (b), and (c) showed the room temperature control effects of rooms 7-9. Room 7 and 8 initially had temperatures of 30.8 °C and 29.5 °C, respectively, with their set temperatures set at 25 °C and 22 °C. After 300 minutes of VAV-ACS operation, the temperatures in both rooms had successfully reached the predetermined standards. Especially room 8, its temperature had dropped to 22 °C after about 45min. The room 9's original temperature was also 30.8 °C, and its target was set at 25 °C. The AV and End Damper Control Effects (EDCE) of different rooms are shown in Figure 11.

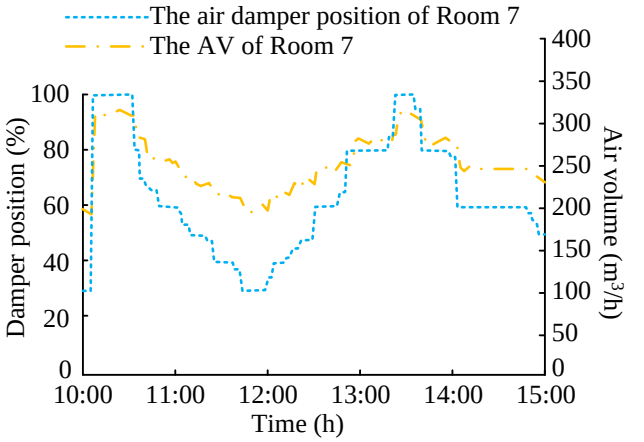

(a) AV and EDCE of room 7

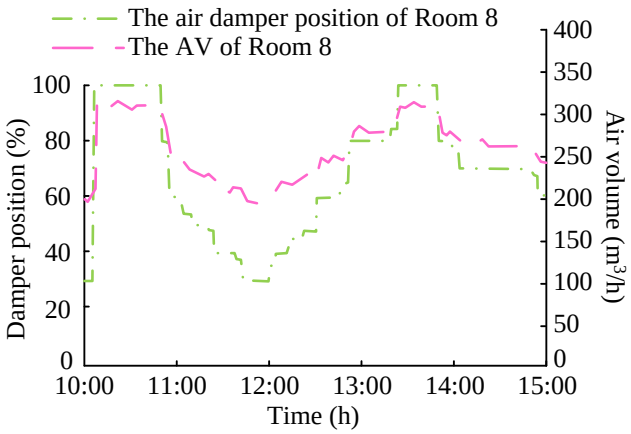

(b) AV and EDCE of room 8

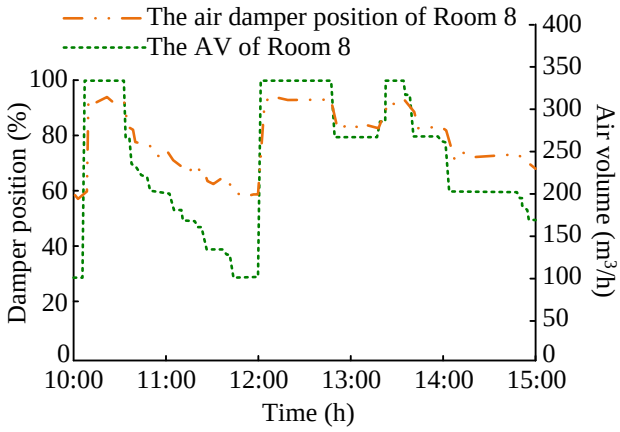

(c) AV and EDCE of room 9

Figure 11: AV and EDCEs in different rooms

Figure 11 (a) showed the effect of AV control and end air valve adjustment in room 7. After 300 minutes of VAV system operation, the room temperature successfully reached the set target. Room 7 firstly reached the set temperature within approximately 30min, but subsequently, due to changes in the indoor environment and fluctuations in the supply air static pressure, the fan speed was adjusted, resulting in fluctuations in the room temperature. Figure 11 (b) showed the air flow control situation in room 8. FCA demonstrated accurate temperature prediction ability, effectively reducing the frequency and amplitude of air valve fluctuations, and maintaining stable InT. This study intentionally opened the room 9's doors and windows between 120 and 180 minutes to increase the heat load, as shown in Figure 11 (c). Despite the sudden increase in InT caused by this, FCA was still able to quickly adjust and accurately predict InT, and adjust the opening of the air valve in a timely manner to change the ASV. Through this real-time adjustment, the FCA control model

ultimately helped room 9 achieve the set temperature target.

5 Discussion

This study has achieved significant results in the intelligent management of VAV-ACS, especially in the improvement of parameter optimization, response speed, energy consumption reduction, and control strategy flexibility. Through the application of DBN models and FCAs, this study achieved lower average absolute relative error and higher coefficient of determination compared to other models in existing literature. Compared with the machine learning combined with improved PSO method proposed by scholars such as He N, the DBN model in this study avoided local optimization problems in parameter optimization and improved generalization ability. The improvement of system response speed was attributed to the accurate description of dynamic characteristics and real-time adjustment ability of FCA. In terms of energy consumption, the precise control in this study reduced energy waste and exhibited better energy-saving effects compared to the dual VAV system proposed by scholars such as Nassif N. The flexibility of control strategies benefited from the algorithm's ability to quickly adapt to changes in indoor and outdoor environments and user needs. The predictive ability of the DBN model and the real-time adjustment ability of the FCA were the main reasons for the breakthrough in MARE and determination coefficient in this study. This provides an efficient and accurate intelligent control method for building energy management.

The proposed solution demonstrates novelty in the field of building energy management by combining a coupled model with DNN. The coupled model improves the accuracy of input data, enabling DNN to capture the complex relationship between building thermodynamic characteristics and indoor environmental changes, thereby significantly reducing prediction errors. Compared with traditional control strategies, the FCA enhances the adaptability and robustness of the system, effectively handling the time-varying input and system dynamics, and achieving more stable and accurate control. The optimized DBN model network structure and parameter adjustment result in enhanced performance. The application of FCA provides a novel approach to VAV system control, particularly in the context of uncertainty and fuzziness.

6 Conclusion

In modern architectural environments, ACS is a key facility for maintaining indoor comfort and air quality. This study applied DBN to optimize hotel VAV-ACS and constructed a mathematical model to analyze heat transfer to improve DBN prediction accuracy. The system dynamically adjusted the air valve based on the predicted temperature difference to achieve precise control of the indoor environment. Simulation experiments showed that InT could be quickly adjusted to OuT, and the DBN model was superior to other neural network models in predicting ASV, with an MARE of 1.555% and a determination coefficient of 0.9975. Actual tests had shown that the room temperature successfully reached the set target within 300 minutes, and FCA performed well in adjusting the air valve and controlling room temperature, maintaining stability even under interference conditions. These results provided effective intelligent control strategies for building energy management. This study mainly focuses on specific working conditions and hotel building environments, which may not fully represent all types of buildings and climate conditions. Further experiments can be conducted in more places.

Funding statement

The research is supported by the Vocational and Technical Education Society Scientific Research Projects of Hubei Province in 2023, "How to Combine CESIM and the core curriculum for Hotel Digitization skills" (No. ZJGB2023059).

References

[1] W. Wang, X. Shan, S. A. Hussain, C. Wang, and Y. Ji, "Comparison of multi-control strategies for the control of indoor air temperature and CO2 with OpenModelica Modeling," Energies, vol. 13, no. 17, pp. 4425-4445, 2020. https://doi.org/10.3390/en13174425

[2] D. Wei, H. Feng, Q. Han, and K. Jia, "Fault detection and diagnosis for variable-air-volume systems using combined residual, qualitative and quantitative techniques," Energy and Buildings, vol. 254 no. 1, pp. 111491.1-111491.17, 2020. https://doi.org/10.1016/j.enbuild.2021.111491

[3] Z. Xia, H. Guan, Z. Qi, and P. Xu, "Multi-zone infection risk assessment model of airborne virus transmission on a cruise ship using CONTAM," Buildings, vol. 13, no. 9, pp. 2350-2370, 2023. https://doi.org/10.3390/buildings13092350

[4] N. Nassif, M. Tahmasebi, I. Ridwana, and P. Ebrahimi, "New optimal supply air temperature and minimum zone air flow resetting strategies for VAV Systems," Buildings, vol. 12, no. 3, pp. 348-363, 2022. https://doi.org/10.3390/buildings12030348

[5] Z. Zhai, H. Li, R. Bahl, and K. Trace, "Application of portable air purifiers for mitigating COVID-19 in large public spaces," Buildings, vol. 11, no. 8, pp. 329-343, 2021. https://doi.org/10.3390/buildings11080329

[6] N. He, K. Xi, M. Zhang, and S. Li, "A novel tuning method for predictive control of VAV air conditioning system based on machine learning and improved PSO," Journal of Beijing Institute of Technology, vol. 31, no. 4, pp. 350-361, 2022. https://doi.org/10.15918/j.jbit1004-0579.2022.039

[7] T. Zhao, J. Wang, C. Liu, and Y. Zhao, "Feasibility

study of retrofitting VAV system to VAV-DOAS system for outdoor airflow requirement and distribution in multi-zone VAV system," Science and Technology for the Built Environment, vol. 27, no. 7, pp. 892-902, 2021. https://doi.org/10.1080/23744731.2020.1865778

[8] N. Nassif and I. Ridwana, "Improving building energy performance using dual VAV configuration integrated with dedicated outdoor air system," Buildings, vol. 11, no. 10, pp. 466-484, 2021. https://doi.org/10.3390/buildings11100466

[9] T. Zhao, J. Wang, C. Liu, P. Hua, Y. Zhou, and Y. Zhao, "Comparative study of outdoor airflow requirement and distribution in multi-zone VAV system with different control strategies," Science and Technology for the Built Environment, vol. 27, no. 4, pp. 489-508, 2020. https://doi.org/10.1080/23744731.2020.1819062

[10] T. Zhao, Z. Li., X. Li, and H. Peng, "Global hydraulic stability analysis for dynamic regulation in multi-zone variable air volume air-conditioning system," Energy and Built Environment, vol. 5, no. 4, pp. 592-606, 2024. https://doi.org/10.1016/j.enbenv.2023.05.001

[11] J. A. Jornet-Monteverde and J. J. Galiana-Merino, "Low-cost conversion of single-zone HVAC systems to multi-zone control systems using low-power wireless sensor networks," Sensors, vol. 20, no. 13, pp. 3611-3639, 2020. https://doi.org/10.3390/s20133611

[12] D. Wei, J. Ma, H. Jiao, and Y. Ran, "Model predictive control for multi-zone Variable Air Volume systems based on artificial neural networks," Journal of Process Control, vol. 118, no. 8, pp. 185-201, 2022. https://doi.org/10.1016/j.jprocont.2022.08.014

[13] L. Yu, Y. Sun, Z. Xu, C. Shen, D. Yue, T. Jiang, and X. Guan, "Multi-agent deep reinforcement learning for HVAC control in commercial buildings," IEEE Transactions on Smart Grid, vol. 12, no. 1, pp. 407-419, 2020. https://doi.org/10.1109/TSG.2020.3011739

[14] Y. Zhao, C. Zhang, Y. Zhang, Z. Wang, and J. Li, "A review of data mining technologies in building energy systems: Load prediction, pattern identification, fault detection and diagnosis," Energy and Built Environment, vol. 1, no. 2, pp. 149-164, 2020. https://doi.org/10.1016/j.enbenv.2019.11.003

[15] S. Yan, L. Wang, M. J. Birnkrant, Z. Zhai, and S. Miller, "Multizone modeling of airborne SARS-CoV-2 quanta transmission and infection mitigation strategies in office, hotel, retail, and school buildings," Buildings, vol. 13, no. 1, pp. 102-126, 2022. https://doi.org/10.3390/buildings13010102

[16] Y. Zhang, T. Yan, X. Xu, and J. Gao, "Room temperature and humidity decoupling control of common variable air volume air-conditioning system based on bilinear characteristics," Energy and Built Environment, vol. 4, no. 3, pp. 354-367, 2023. https://doi.org/10.1016/j.enbenv.2022.02.005

[17] R. S. Dornelas and D. A. Lima, "Correlation filters in machine learning algorithms to select De-mographic and individual features for autism spectrum disorder diagnosis," Journal of Data Science and Intelligent Systems, vol. 3, no. 1, pp. 7-9, 2023. https://doi.org/10.47852/bonviewJDSIS32021027

[18] N. Asim, M. Badiei, and M. Mohammad, "Sustainability of heating, ventilation and air-conditioning (HVAC) systems in buildings-An overview," International Journal of Environmental Research and Public Health, vol. 19, no. 2, pp. 1016-1032, 2022. https://doi.org/10.3390/ijerph19021016

[19] A. Bakker, J. A. Siegel, M. J. Mendell, and A. J. Prussin, "Bacterial and fungal ecology on air conditioning cooling coils is influenced by climate and building factors," Indoor Air, vol. 30, no. 2, pp. 326-334, 2020. https://doi.org/10.1111/ina.12632

[20] A. Makar, S. Mahmoud, R. Al-Dadah, M. Ismail, and M. Almesfer, "Impact of ambient temperature and humidity on the performance of vapour compression air conditioning system-experimental and numerical investigation," CFD Letters, vol. 16, no. 7, pp. 1-21, 2024. https://doi.org/10.37934/cfdl.16.7.121